 doi:10.20944/preprints202105.0631.v1

On the relationship between Circulation patterns, the Southern Annular Mode, and rainfall variability in Western Cape

Chibuike Chiedozie Ibebuchi

Institute of Geography and Geology, University of Würzburg, Am Hubland, 97074 Würzburg, Germany

Corresponding author's email: chibuike.ibebuchi@uni-wuerzburg.de

Abstract

This study investigates circulation types (CTs) in Africa, south of the equator, that are related to wet and dry conditions in Western Cape, the statistical relationship between the selected CTs and the Southern Annular Mode (SAM), and changes in the frequency of occurrence of the CTs related to the SAM under the ssp585 scenario. Obliquely rotated principal component analysis applied to sea level pressure was used to classify CTs in Africa, south of the equator. Three CTs were found to have a high probability to be associated with wet days in Western Cape, and four CTs were equally found to have a high probability to be associated with dry days in Western Cape. Generally, the dry/wet CTs feature the southward/northward track of the mid-latitude cyclone, adjacent to South Africa; anti-cyclonic/cyclonic relative vorticity, and poleward/equatorward track of westerlies, south of South Africa. One of the selected wet CTs is significantly related to variations of the SAM. Years with an above-average SAM index correlate with the below-average frequency of occurrence of the wet CT. The results suggest that through the dynamics of the CT, the SAM might control the rainfall variability of Western Cape. Under the ssp585 scenario, the analyzed climate models indicated a possibility in the decrease of the frequency of occurrence of the aforementioned wet CT associated with cyclonic activity at the mid-latitudes, and an increase in the frequency of occurrence of the CT associated with enhanced SLP in the mid-latitudes.

Keywords: Western Cape, Southern Annular Mode, Circulation type, Africa south of the equator, mid-latitude cyclone

Introduction

The Southern Annular Mode (SAM) is a low-frequency mode of atmospheric variability of the southern hemisphere. The SAM is characterized by a zonally symmetric north-south movement of the westerly belt that encircles Antarctica (Thompson and Wallace 2000). Its positive phase features: a southward shift of the westerly belt, enhanced mean sea level pressure (SLP) in the mid-latitudes, and lower SLP, in the high latitudes; the opposite occurs during its negative phase. According to Watterson (2001), the existence of the SAM is mostly due to internal atmospheric dynamics. North-south migration of storm tracks in the southern hemisphere which is related to sea surface temperature (SST) variability (Screen et al. 2009)

 doi:10.20944/preprints202105.0631.v1

and mid-latitude precipitation variability (Hendon et al. 2007) can be associated with variations of the SAM (Condron 2005). According to Hall and Visbeck (2002) variations of the SAM can also influence ocean circulation.

Seager et al. (2003) reported that variability of the SAM on an inter-annual time scale is partly related to the El Niño Southern Oscillation (ENSO) during the austral summer; the negative SAM is related to El Niño and the positive SAM to La Niña. Wang and Cai (2013) noted that the positive phase of ENSO which increases the global mean sea surface temperature contributes to the negative phase of SAM. According to L'Heureux and Thompson (2006), during austral summer, about 25% of the variance of the SAM is related to ENSO variations. Thus Ding et al. (2012) explained that the SAM index reflects the superposition of both high-latitude and tropically forced variability.

Under global warming, the SAM is projected to undergo a trend towards positive polarity during austral summer, due to an increase in greenhouse gas concentrations and stratospheric ozone depletion (Gillett and Thompson 2003). Abram et al. (2014) also reported that since the fifteenth century, the SAM has undergone a progressive shift towards its positive phase leading to the warming of the Antarctic Peninsula.

The SAM which accounts for about 20%-30% of the total monthly SLP variability, south of 20°S (Thompson and Wallace 2000), is equally associated with cold fronts and storms which move from west to east (Cai et al. 2011). Studies have investigated the relationship between variations of the SAM and regional land-based precipitation variability of Australia (e.g. Hendon et al. 2007; Cai et al. 2011) and the western parts of South Africa (e.g. Reason and Rouault 2005; Mahlalela et al. 2019). Reason and Rouault (2005) found that negative SAM correlates with wet conditions over western South Africa and vice versa for positive SAM. Since some regions in the Western Cape are characterized by the Mediterranean type of climate, the SAM is expected to influence the patterns of atmospheric circulation that control the rainfall variability of the region. Moreover, the region currently experienced years of decreased rainfall (Muller 2018), and variations of the SAM might further increase the vulnerability of the region, making it necessary for a deeper understanding of the hydroclimate of the region, and enhanced predictability of rainfall in the region.

Using Self Organising Map (SOM) Engelbrecht and Landman (2016) investigated the link between the inter-annual variability of seasonal rainfall over the Cape south coast of South Africa and circulation types. Compared to hard clustering algorithms (e.g. K-means clustering), the SOM performs relatively better in synoptic classifications since it can generate non-linear classification (Philippopoulos et al. 2014). However, given that atmospheric circulation is a continuum, the probability of group membership is an important factor that contributes to the relatively high accuracy of synoptic classifications and this is achieved by (fuzzy) classification schemes (e.g. rotated principal component analysis (PCA)) that allow overlapping of the classified variable (Richman and Gong 1999; Xu and Tian 2005; Ibebuchi 2021b). When applied to a climatic field represented in the T-mode structure (i.e. variable is time series and observation is grid points), rotated T-mode PCA has proved to be a useful tool in circulation typing (Richman 1981, 1986; Huth 1996; Compagnucci et al. 2001). According to Compagnucci et al. 2001 "*T-mode proved to be a useful tool for extracting and reproducing the circulation types, quantifying their frequency and showing the dominant weather periods in them".* The added values of this work are (i) the application of a fuzzy clustering scheme at a larger domain to investigate CTs related to wet and dry conditions in Western Cape and if any of the CTs relates to the SAM, (ii) the analysis of changes in the annual frequency of occurrence of the CTs related to the SAM using CMIP6

Preprints (www.preprints.org) | NOT PEER-REVIEWED | Posted: 26 May 2021 doi:10.20944/preprints202105.0631.v1

GCMs for the updated ssp585 scenario. Thus using a circulation typing technique known to reproduce the synoptic situations in a study region, for the separation of wetting and drying signals in Western Cape, and relating the signals to the SAM, this work strengthens existing studies (e.g. Muller 2018; Otto et al. 2018; Wolski 2018; Burls et al. 2019) on addressing the dynamics associated with rainfall changes in the Western Cape under the current climate and under future climate change, using the current ssp585 scenario.

2 Data and Methodology

SLP; relative vorticity and wind vector at 850 hPa data sets are obtained from ERA5 reanalysis (Hersbach et al. 2020). The horizontal resolution of the data sets is 0.25° longitude and latitude and the temporal resolution is daily from 1979-2019. The gridded Precipitation data set is obtained from the Climate Prediction Centre (CPC) (Xie et al. 2007) at a horizontal resolution of 0.5° longitude and latitude. Station data over Western Cape is obtained from http://www.dwa.gov.za/Hydrology/Verified/hymain.aspx. The temporal resolution of the precipitation data sets is daily from 1979-2019. Since the quality controlled station data over Western Cape for the 1979-2019 period are sparsely distributed, the station data is rather used to validate daily rainfall estimates from CPC over Western Cape for the 1979-2019 period. SLP data sets are obtained from two CMIP6 general climate models (GCMs), which were pre-selected due to their capability to simulate the statistical properties of interest of the CTs related to the SAM. The GCMs are MPI-ESM-LR and EC-EARTH3-CC. The SLP data sets are obtained for the historical experiment (1979-2014) and the ssp585 scenario (2050-2100) which is an update of the RCP8.5 scenario and is characterized with emissions high enough to produce the $8.5\,W/m^2$ level of forcing in 2100.

The spatial extent for the circulation typing is 0-50.25°S and 4°E-55.25°E. The inclusion of the tropics is based on the finding of Grassi et al. (2005) that SST forcing at the tropics during austral summer can impact the SAM by modifying the planetary waves and the mid-latitude jet. Also, the adjacent oceans surrounding southern African landmasses act as moisture sources (Cook 2000), thus they were included to the spatial extent that inshore moisture transport is plausible. The selected target region captures the major rain-bearing synoptic systems in the study domain such as the northeast cross-equatorial trade winds, the semi-permanent high-pressure system, the Angola low, the mid-latitude cyclones (during its northward track), the Mozambique Channel trough, etc.

Obliquely rotated PCA (Richman 1981) is used in classifying the CTs in the study region. It is applied to the T-mode matrix of daily z-score standardized SLP data set from 1979 to 2019. The SLP data set, according to Kidson (1997), provides a good representation of synoptic-scale systems and explains the relationship between topography and low-level flow. He further noted that between 1000 hPa to 500 hPa, the choice of the level to use in the classification has little influence on the explanation of surface variables. According to Compagnucci et al. (2001) "*The T-mode analysis can lead to the determination of frequent synoptic situations, improving the basic knowledge essential to weather forecasting, among other things. The application of such a tool to a wide range of processes, ranging from the daily synoptic developments to the monthly or annual mean developments is valuable for an ample set of atmospheric processes, including both daily variability and climate fluctuations and change".* Thus in addition to the usefulness of this clustering approach to reproduce synoptic situations known *a priori* in a given domain and quantifying their frequency of occurrence and dominant periods, its applicability in studying climate fluctuations and

Preprints (www.preprints.org) | NOT PEER-REVIEWED | Posted: 26 May 2021 doi:10.20944/preprints202105.0631.v1

change makes it a good candidate for the study purpose since the classification scheme is applied also to GCMs under the historical and future climate change scenario.

The time series are related using the correlation matrix, and singular value decomposition is used to obtain the eigenvalues and the eigenvectors. The eigenvectors are weighted with the square root of their corresponding eigenvalues which make them longer than a unit length, henceforth referred to as loadings (Richman and Lamb 1985). The number of components to retain is based on the recommendation of North et al. (1982) on the separation of the eigenvalues and sensitivity analysis. The sensitivity analysis ensures that after components with typically high and separated eigenvalues were retained, the addition of a further component uncovers a new input pattern that has not been delineated by previous vectors (Richman 1981). This was assessed by rotating the components iteratively and assessing the goodness of match based on the congruence coefficient between the vectors, and visual inspection of the map patterns (Richman 1986; Barriera and Compganucci 2011). The oblique rotation made at a power of 2 with Promax, eliminates orthogonality constraint and maximizes the number of near-zero loadings so that each retained component clusters unique days with a similar input pattern (Richman 1986). To enhance the coherency between the weather patterns clustered under each class, a subjective threshold of ± 0.2 (Richman and Gong 1999) is used to further cluster the loading in each retained component to negative high loadings and positive high loadings so that each retained component forms two classes. The mean SLP for the days clustered under each class is the CT. Detailed justifications of all the subjective decisions followed in the classification process and the fuzziness of the approach are explained in detail by Ibebuchi (2021b).

The probability of each CT to bring dry days (daily rainfall amount <1mm) or wet days (daily rainfall amount>1mm) across each grid in Western Cape is assessed using Eq. 1 and 2.

$$P_{d_i} = \frac{d_i}{N_i} \times 100 \quad i = 1 \ldots n \tag{1}$$

$$P_{w_i} = \frac{w_i}{N_i} \times 100 \quad i = 1 \ldots n \tag{2}$$

P_{d_i} is the percentage of dry days for a given CT; d_i is the total number of dry days for the CT in question; N_i is the total number of days clustered under a given CT. $P_{w_i}$is the percentage of wet days in a given CT, and w_i is the total number of wet days for the CT in question and n is the number of CTs classified.

Since CTs are naturally fuzzy and overlap, a given CT is not confined to occur at a specific season. However, the seasonality of CTs that are selected to have a high probability to bring wet days or dry days across the majority of a majority of the grid points in Western Cape is analyzed to uncover if the CTs tend to be dominant at a specific season(s). The dominant period of a given CT is equally when its signal is most likely to be well expressed due to its persistence for a longer period. Thus, rainfall anomaly at each grid point for the season when the CT is most expressed is calculated with respect to the climatology of the season. The anomalies are tested for statistical significance using the non-parametric permutation test. Wind vectors and relative vorticity composites at 850 hPa are used to further analyze the operational mechanism of the CTs that relates them to wet and dry days in

Preprints (www.preprints.org) | NOT PEER-REVIEWED | Posted: 26 May 2021 doi:10.20944/preprints202105.0631.v1

Western Cape. The 850 hPa height is used since according to Reason and Smart (2015) it is the height above the interior plateau that exists over much of southern Africa.

The SAM index is obtained from https://climatedataguide.ucar.edu/climate-data/marshall-southern-annular-mode-sam-index-station-based, for the 1979-2019 period. Correlation analysis is used to relate the time series (loadings) of the CTs with a higher probability to bring dry condition and wet condition in Western Cape, and the SAM index. Statistical significance of the relationship is assessed at a 95% confidence level using the Kendall-Tau test which is non-parametric. The trend in the annual frequency of occurrence of the CTs related to the SAM is examined under the ssp585 scenario and the statistical significance of the trend is examined using the Mann-Kendall test (Mann 1945; Kendall 1975) for linear trends.

3 Results

3.1 Seasonal rainfall climatology in Western Cape

Fig. 1 exemplifies the annual cycle of rainfall as observed from the station data and the counterpart grid from the CPC data set. For all the stations analyzed, the CPC data set captures the annual cycle of rainfall in Western Cape. However, there is relatively better agreement between the rainfall estimates from the two data sets for the austral spring (SON) and austral summer (DJF) months. During austral autumn (MAM) and austral winter (JJA) CPC significantly underestimates rainfall compared to the other seasons. The same pattern of the result as presented in Fig. 1 was obtained for all the stations analyzed (not shown). Thus while the CPC data set captures the annual cycle of rainfall in Western Cape, it underestimates rainfall from austral autumn to early austral spring (September) relative to the analyzed station data.

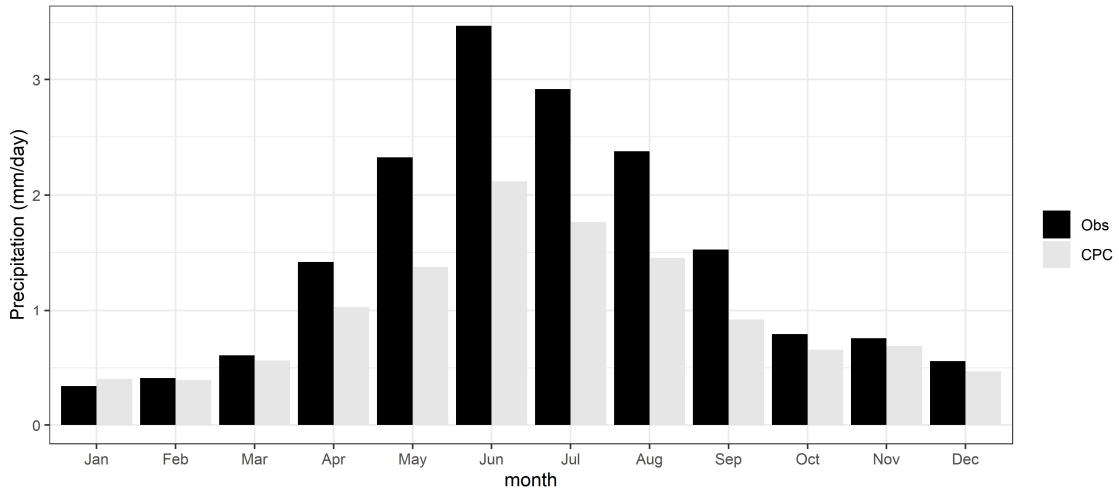

Fig. 1: Annual cycle of rainfall from station data and CPC data set for the 1979-2020 period

From Fig. 2, the spatial rainfall average over the western regions and the northeastern regions of Western Cape exhibits strong seasonality during austral summer and austral winter. During austral summer the western regions are relatively drier, especially the northwestern regions. During austral winter the southwestern regions receive the highest

Preprints (www.preprints.org) | NOT PEER-REVIEWED | Posted: 26 May 2021 doi:10.20944/preprints202105.0631.v1

rainfall amount while the northwestern regions receive lower rainfall amount. Generally, during austral summer (winter) rainfall amount increases from west to east (east to west). During austral autumn rainfall tends to be relatively widespread, while during austral spring a meridional pattern of rainfall can be seen - the northern regions are relatively drier compared to the southern regions.

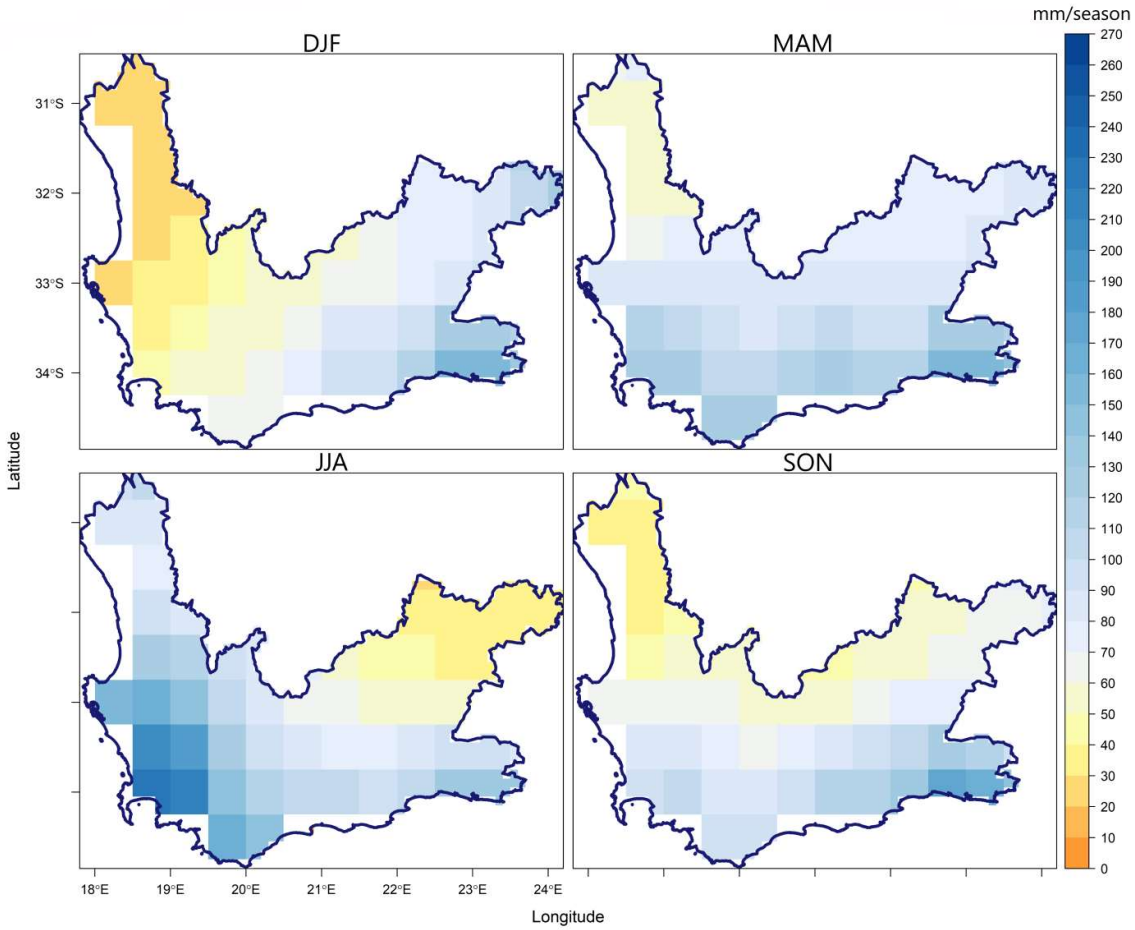

Fig 2: Seasonal climatology of rainfall from CPC data set for the 1979-2020 period

3.2 Circulation types in Africa south of the equator linked to wet and dry days in Western Cape

Fig. 3 shows the CTs classified by retaining 9 optimal components. Each retained component yields two CTs – clusters of positive loadings and negative loadings above the 0.2 threshold. Each CT reveals a large-scale pattern of atmospheric circulation in Africa, south of the equator. Here the focus is on CTs that are associated with wet and dry days in Western Cape, which is marked in Fig. 3 by the blue polygon, situated at the southernmost tip of southern Africa. Fig. 4 shows the probability of the CTs to be associated with wet days (top panel) and dry days (bottom panel) as calculated from Eq. 1 and 2. Based on the 90% percentile threshold value of the probabilities, and the number of grid points with statistically significant wet and dry rainfall anomalies under the active state of each of the CTs, CT3-, CT4- and CT8+ were selected to have the highest probability to bring wet conditions in

Preprints (www.preprints.org) | NOT PEER-REVIEWED | Posted: 26 May 2021 doi:10.20944/preprints202105.0631.v1

Western Cape. On the other hand, CT4+, CT5-, CT7- and CT8- were selected to have the highest probability to bring dry conditions in Western Cape. The dry (wet) CTs are marked by the red (blue) frame in Fig. 3. Fig. 3 shows that for the wet CTs, the mid-latitude cyclone tends to track further north towards the south of South Africa; while for the dry CTs the mid-latitude cyclones are blocked by the subtropical high-pressure system.

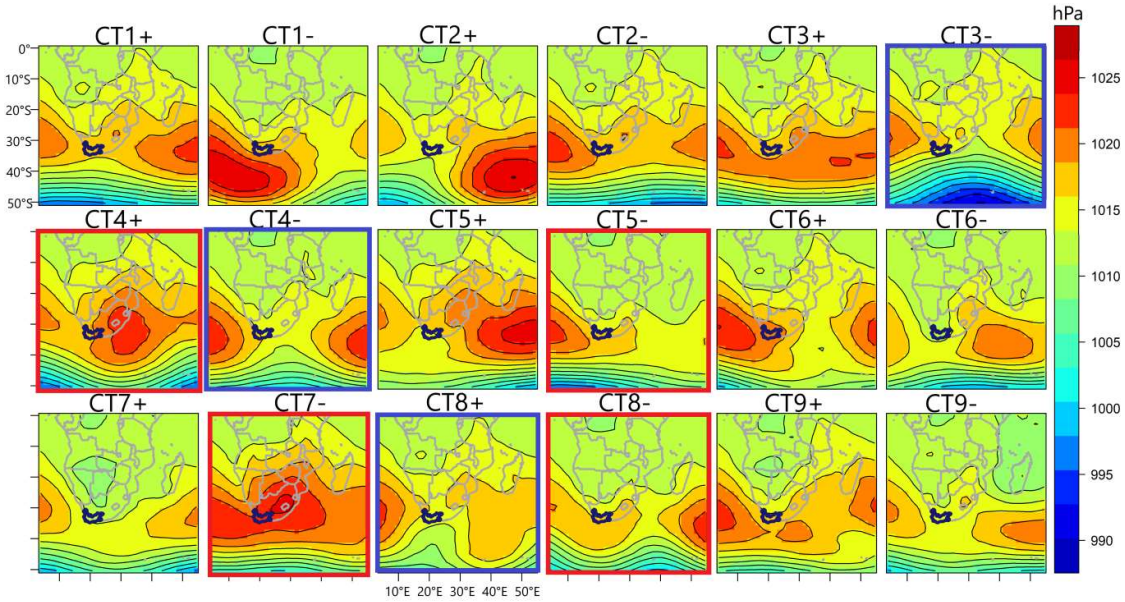

Fig 3: Circulations types in the study region. The CTs is presented by the mean SLP field of the clustered days. Wet (dry) CTs in Western Cape are marked by the blue (red) frames. The blue polygon in the map delineates the position of Western Cape

Preprints (www.preprints.org) | NOT PEER-REVIEWED | Posted: 26 May 2021 doi:10.20944/preprints202105.0631.v1

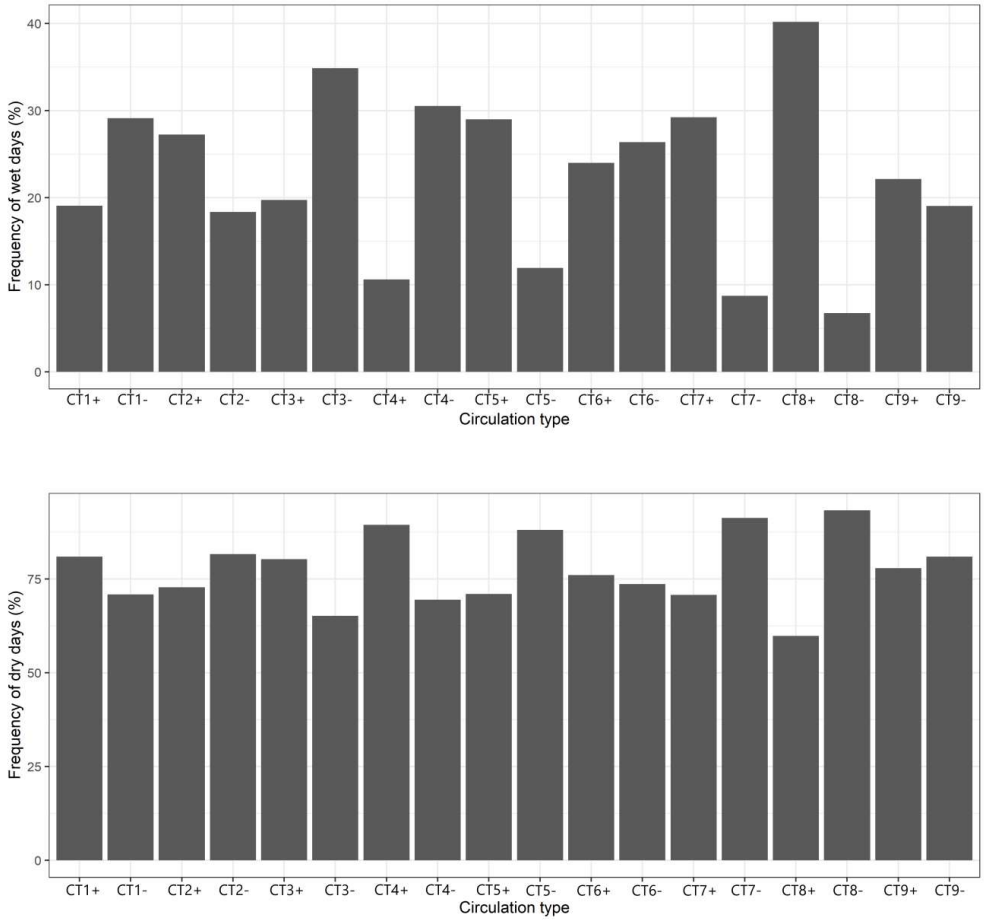

Fig 4: Probability of wet days (top panel) and dry days (bottom panel) associated with the CTs in Fig. 3

From Fig. 5, all the selected CTs except CT8+ tend to exhibit seasonality. For the dry CTs, CT4+, and CT7- tend to prevail during late austral autumn and austral winter. From Fig. 3, both CTs feature dominance of the subtropical anticyclone over southern African landmasses (an indication of a stable atmosphere), with the inclusion of Western Cape. Their circulation features reflect the suppression of moist convection by large-scale subsidence and blocking of the mid-latitude cyclones. In general, they present large-scale circulation features that lead to the suppression of rainfall in Western Cape during austral winter. From Fig. 6, the pattern of rainfall anomaly from CT4+ and CT7- is similar – rainfall is significantly suppressed in the southwestern regions. Also, from Fig. 7, anti-cyclonic vorticity is evident south of South Africa, and over the Greater Agulhas region. Westerlies are equally blocked from progressing northward.

Preprints (www.preprints.org) | NOT PEER-REVIEWED | Posted: 26 May 2021 doi:10.20944/preprints202105.0631.v1

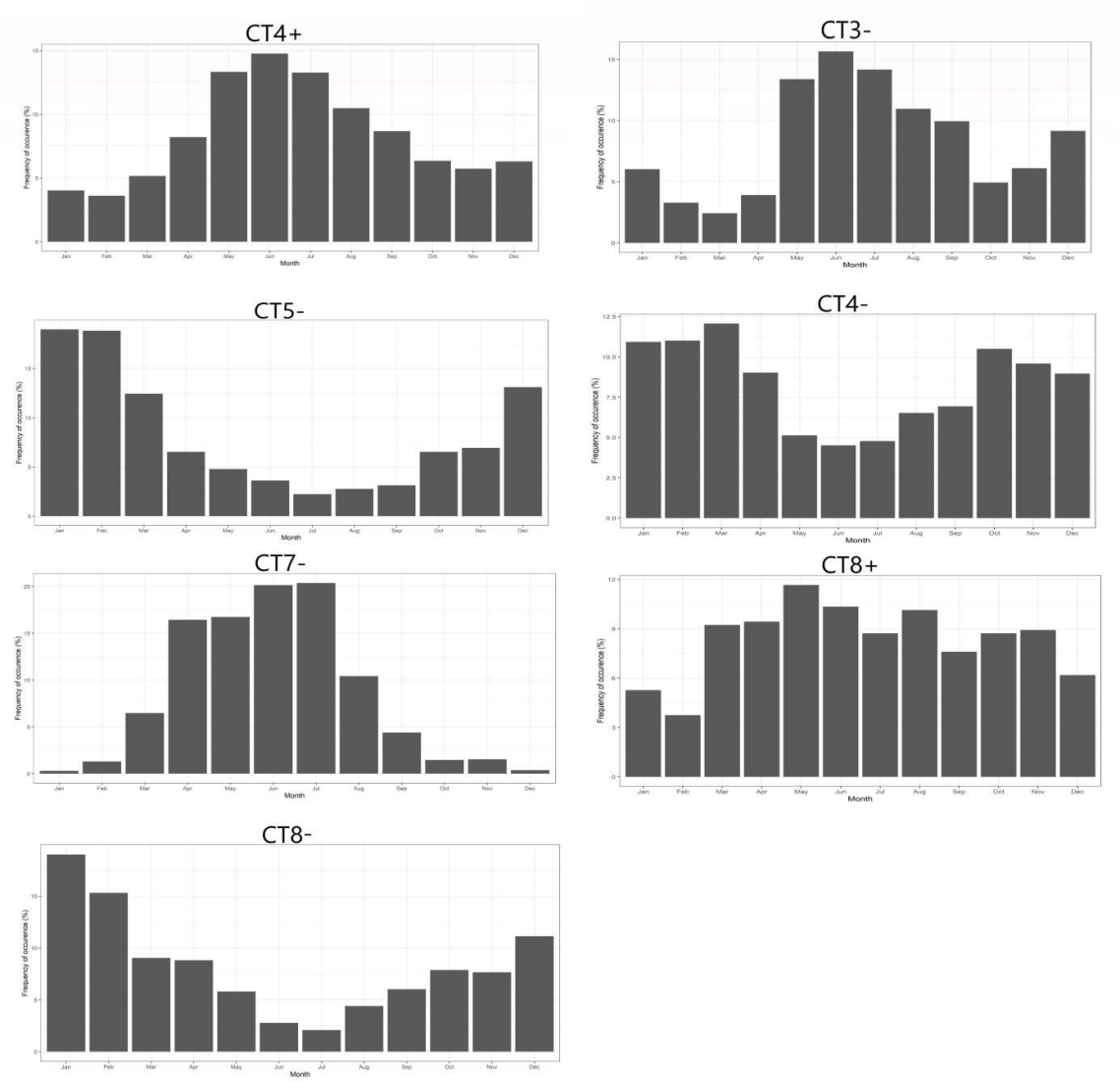

Fig. 5: Annual cycle of the selected CTs associated wet days (right panel) and dry days (left panel) in Western Cape

Preprints (www.preprints.org) | NOT PEER-REVIEWED | Posted: 26 May 2021 doi:10.20944/preprints202105.0631.v1

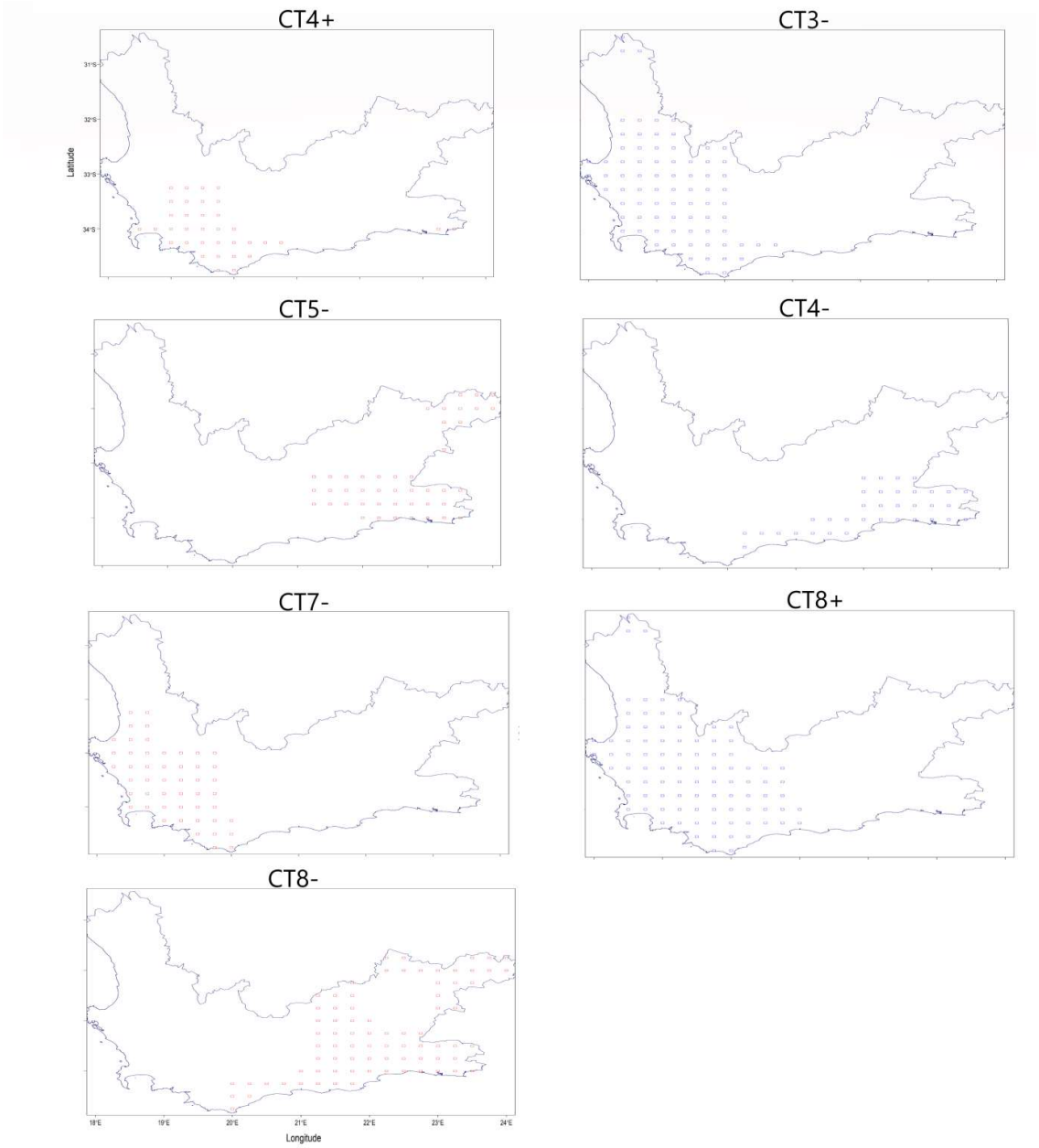

Fig 6: Rainfall anomaly associated with wet CTs and the dry CTs. The anomaly was calculated as the difference between the season the CTs are dominant and the climatology of the season. Blue (red) boxes indicate grid points with statistically significant positive (negative) rainfall anomalies. The dry (wet) patterns are in the left (right) panel

Preprints (www.preprints.org) | NOT PEER-REVIEWED | Posted: 26 May 2021 doi:10.20944/preprints202105.0631.v1

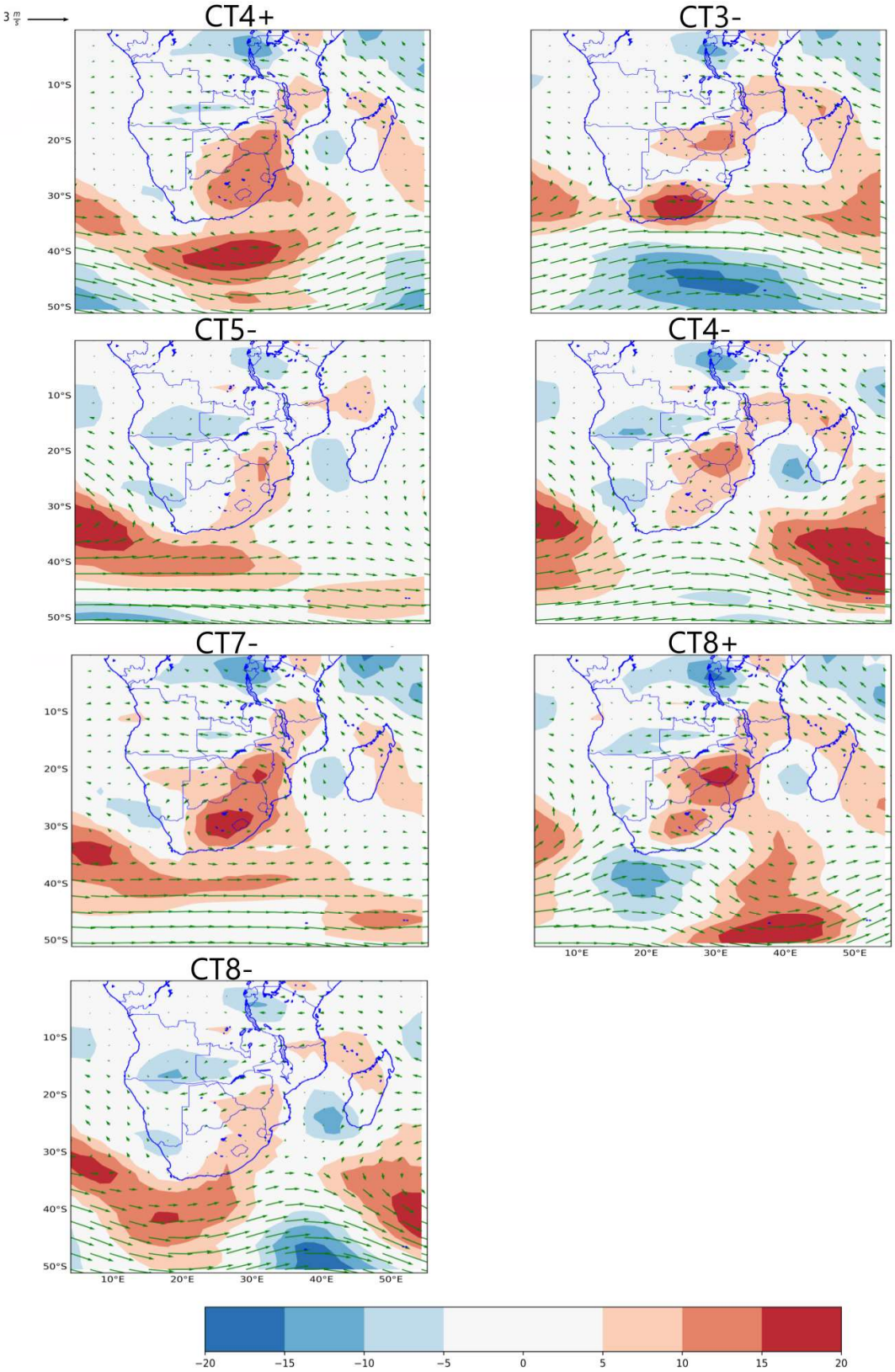

Fig. 7: Composites of wind vector and relative vorticity at 850 hPa for the selected CTs. The

Preprints (www.preprints.org) | NOT PEER-REVIEWED | Posted: 26 May 2021 doi:10.20944/preprints202105.0631.v1

scale of wind is given on top of the map. The color bar is relative vorticity with the unit in $10^6 s^{-1}$. Green Vectors is wind. The dry (wet) patterns are in the left (right) panel

CT5- and CT8- are dominant during austral summer. In both CTs, the western branch of the Mascarene high is relatively weakened, and the South Atlantic anticyclone stretches adjacent to South Africa. A more southward position of the subtropical high during austral summer is common; however, the weakening/strengthening of the Mascarene high can be related to ENSO events – El Niño tends to weaken the Mascarene high (Cook 2000); and Type 5 (CT5+/CT5-) was found to be significantly correlated with the Nino3.4 Index (R= 0.38), in such a way that above-average Nino 3.4 index (El Niño) relates with CT5-, suggesting that during strong El Niño events, the weakening of the western branch of the Mascarene high and the associating fluxes of southeasterlies might lead to below-average austral summer rainfall in parts of the eastern regions of Western Cape (Fig. 6). CT8- shows a deformation (southward push) of the mid-latitude cyclone by the South Atlantic subtropical anticyclone. The rainfall anomaly from both CTs (Fig. 6) is similar – parts of the eastern regions are significantly dry; generally, this might be linked to the weakening of easterly winds that advect moisture onto the eastern parts of Western Cape from the southwest Indian Ocean. Also, anti-cyclonic vorticity is equally evident south of South Africa; the mid-latitude cyclones and associating band of westerlies are moved further south (Fig. 7).

For the seasonality of the wet patterns, CT3- is dominant from late austral autumn to early austral spring. CT4- tends to dominate mainly in austral summer and also austral spring. Reason and Rouault (2005) reported that anomalous circulation patterns that control the austral winter rainfall variability of Western Cape extend into austral spring. CT8+ tends to dominate during May, it nevertheless has a high probability to occur throughout the seasons except for austral summer. The mid-latitude disturbance tracks northward and is equally well expressed under CT3- (Fig. 3), a band of westerlies is equally enhanced northward (Fig. 7), allowing cold fronts to sweep across Western Cape; also cyclonic vorticity is evident south of South Africa; as a result, rainfall is significantly enhanced at western regions of Western Cape (Fig. 6). Positive rainfall anomaly under CT4- is statistically significant in parts of the southeastern regions, and in the western regions under CT8+. The circulation features for both CTs are similar to CT3- with respect to cyclonic relative vorticity south of South Africa, and enhanced northward track of westerly winds. However, under CT8+, which has the highest probability to bring wet days to Western Cape, a well-defined cyclonic circulation with the associating westerly wind is evident, just south of Western Cape. Unlike its inverse (i.e. CT8-) the deformation of the mid-latitude cyclone by the subtropical ridge, in this case, favors the northward track of the cyclone towards Western Cape.

Relationship between the selected circulation types and the Southern Annular Mode

Correlation analysis between the loadings of the Types selected to be associated with wet and dry conditions in Western Cape and the SAM revealed that the SAM is significantly related to Type 3 (R=0.46). On the monthly scale, the relationship was found to be strongest in December. From Fig. 3, Type 3 (i.e. CT3+/CT3-) features the southward/northward track of the mid-latitude cyclone. It can be generalized that the negative phase of SAM is related to CT3-, while the positive phase of SAM is related to CT3+ and this relationship is physically justified given the southward/northward track of mid-latitude cyclones during positive/negative phases of the SAM. The time series of the loadings of Type 3 and the SAM is shown in Fig. 8 for 1979-2019; it can be seen that the variations of the SAM can be highly related to this input pattern at the inter-annual time scale, and through the dynamics of Type

Preprints (www.preprints.org) | NOT PEER-REVIEWED | Posted: 26 May 2021 doi:10.20944/preprints202105.0631.v1

3, the SAM can modulate wet and dry days in Western Cape. Interestingly, CT3+ is also the austral summer climatology of atmospheric circulation in Africa, south of the equator (Ibebuchi 2021a) – i.e. it is the most frequent and persistent austral summer pattern.

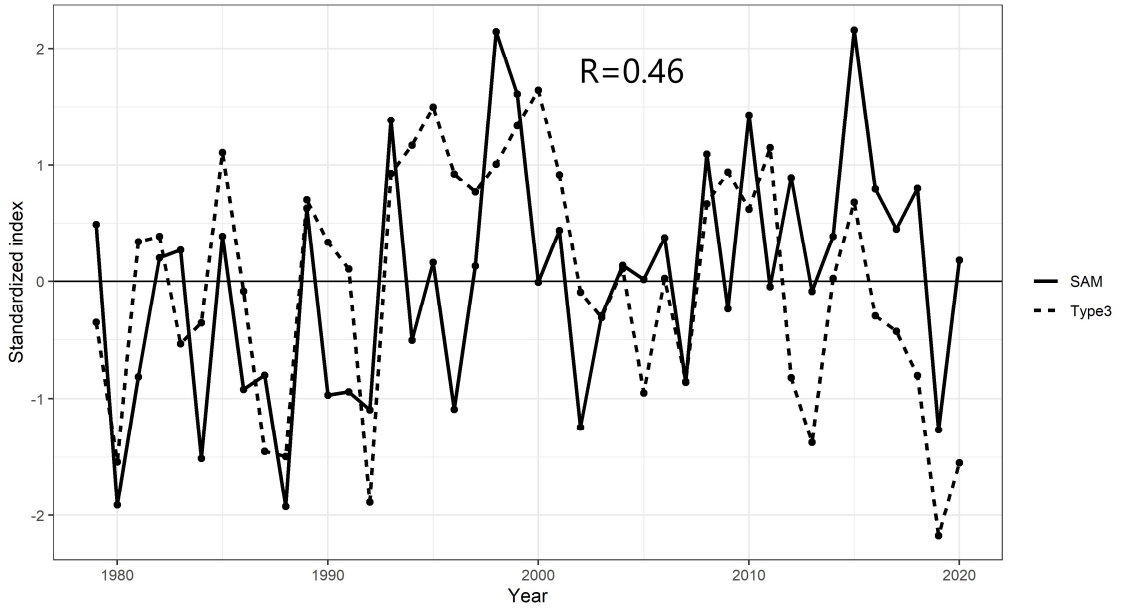

Fig. 8: Time series of the SAM, Type 3 for the 1979-2020 period. The correlation coefficient between the indices is written in the graph.

Fig. 9 shows that years with above-average SAM index can be significantly associated with above-average frequency of occurrence of CT3+ but the below-average frequency of occurrence of CT3-. On the other hand, years with below-average SAM index can be associated with below-average frequency of occurrence of CT3+ but the above-average frequency of occurrence of CT3-.

Preprints (www.preprints.org) | NOT PEER-REVIEWED | Posted: 26 May 2021 doi:10.20944/preprints202105.0631.v1

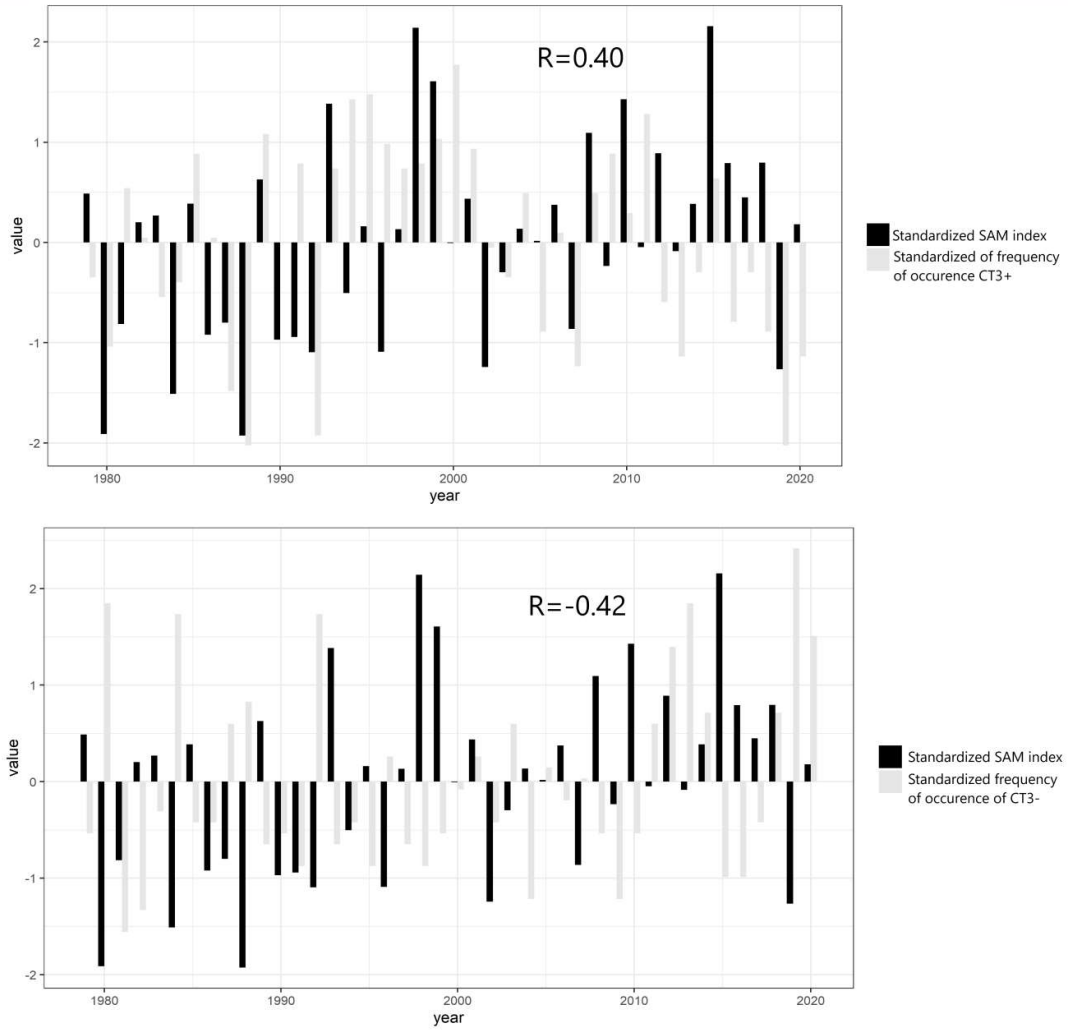

Fig. 9: Relationship between the annual frequency of occurrence of CT3+ (top panel) and CT3- (bottom panel) and the SAM for the 1979-2020 period. The correlation coefficient between the indices is written in the graph.

The classification scheme was applied to the selected GCMs, under the historical and ssp585 experiments, and the input patterns and corresponding CTs were reproduced in all cases, with a one to one correspondence - based on the congruence coefficient between the scores and visual inspection of the maps (c.f. Fig. 11). Fig. 10 shows that under the historical experiment, the GCMs faithfully capture the annual frequency of occurrence of CT3+ and CT3-, though on average, it tends to overestimate/underestimate the frequency of CT3-/CT3+. Based on the Mean absolute error, MPI-ESM captures the annual occurrence of the CTs as obtained from ERA5, compared to EC-Earth. Fig. 11 exemplifies from the EC-Earth model the CTs as classified under the ssp585 scenario. It can be seen that even under greenhouse gas warming, the climate models can reproduce the CTs as obtained from ERA5 in Fig. 3. Thus the CTs are integral parts of the underlying physics in the SLP data sets in the study region, regardless of the analysis period, choice of an appropriate data set (e.g. Ibebuchi 2021a), and climatic condition. The CTs related to the positive/negative SAM are marked by

Preprints (www.preprints.org) | NOT PEER-REVIEWED | Posted: 26 May 2021 doi:10.20944/preprints202105.0631.v1

the red/blue frames. Under the ssp585 scenario, a statistically significant positive trend was found in the frequency of occurrence of CT3+ for both GCMs, indicating that the frequency of enhanced SLP at the mid-latitudes might increase under climate change. The trend in CT3- is negative and statistically significant for the EC-Earth GCM. Even though the negative trend in CT3- is not significant under the MPI-ESM model for the 2050-2100 analysis period, when the analysis period is extended to start from 2030 or below, the trend becomes statistically significant, suggesting that the frequency at which CT3- brings above-average rainfall in the western parts of Western Cape might reduce under green-house gas-induced radiative heating, towards the end of the 21st century.

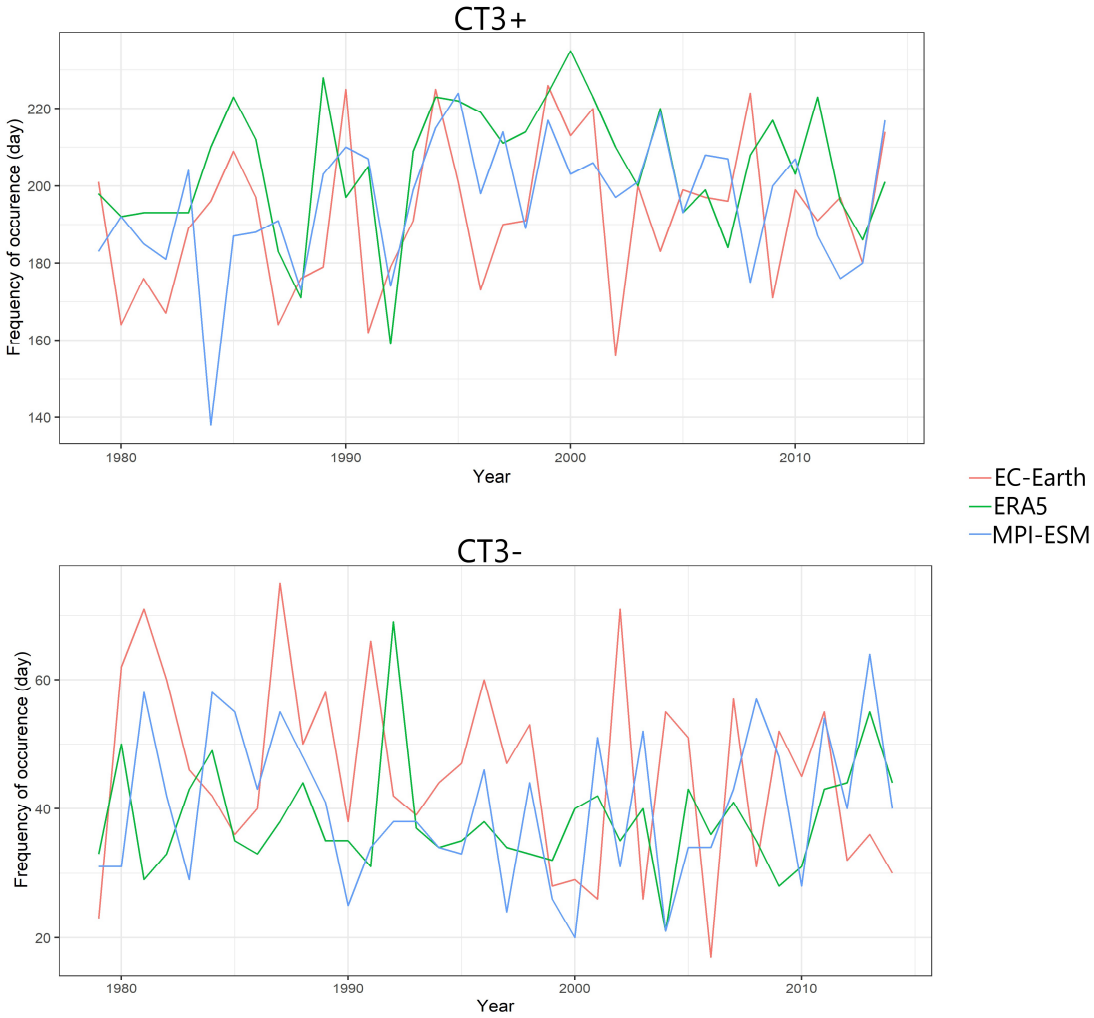

Fig. 10: Validation of the annual frequency of occurrence of CT3+ and CT3- as simulated from the GCMs compared to NCEP for the 1979-2005 period

Preprints (www.preprints.org) | NOT PEER-REVIEWED | Posted: 26 May 2021 doi:10.20944/preprints202105.0631.v1

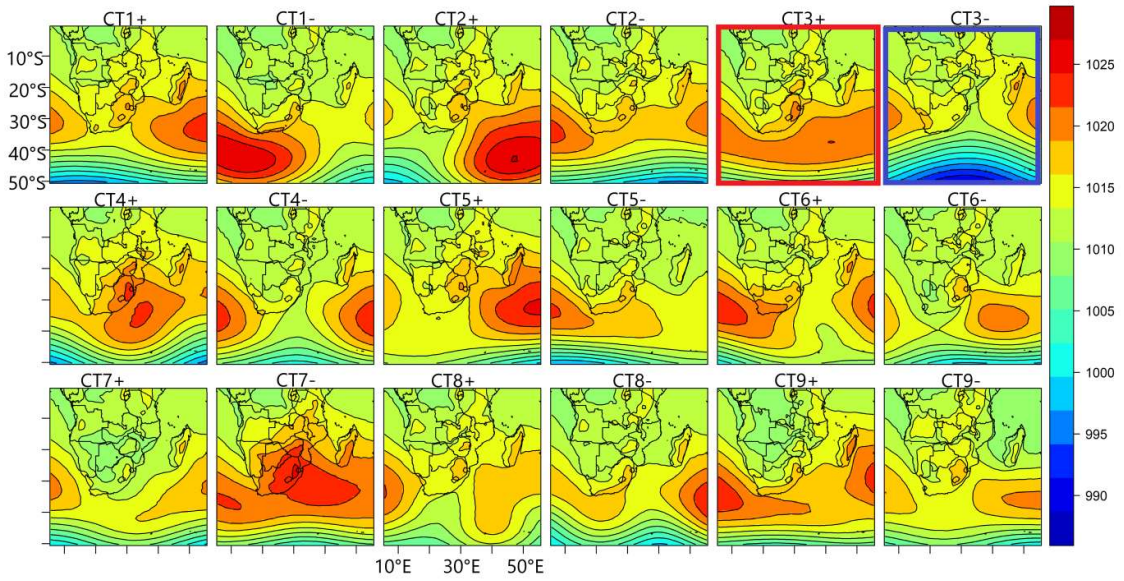

Fig. 11: Circulation types classified from the EC-Earth GCM in the ssp85 experiment for the 2050-2100 period. The selected wet Type related to the SAM is highlighted by the red frame (i.e CT related to the positive SAM) and blue frame (i.e the CT related to the negative SAM). SLP is in hPa.

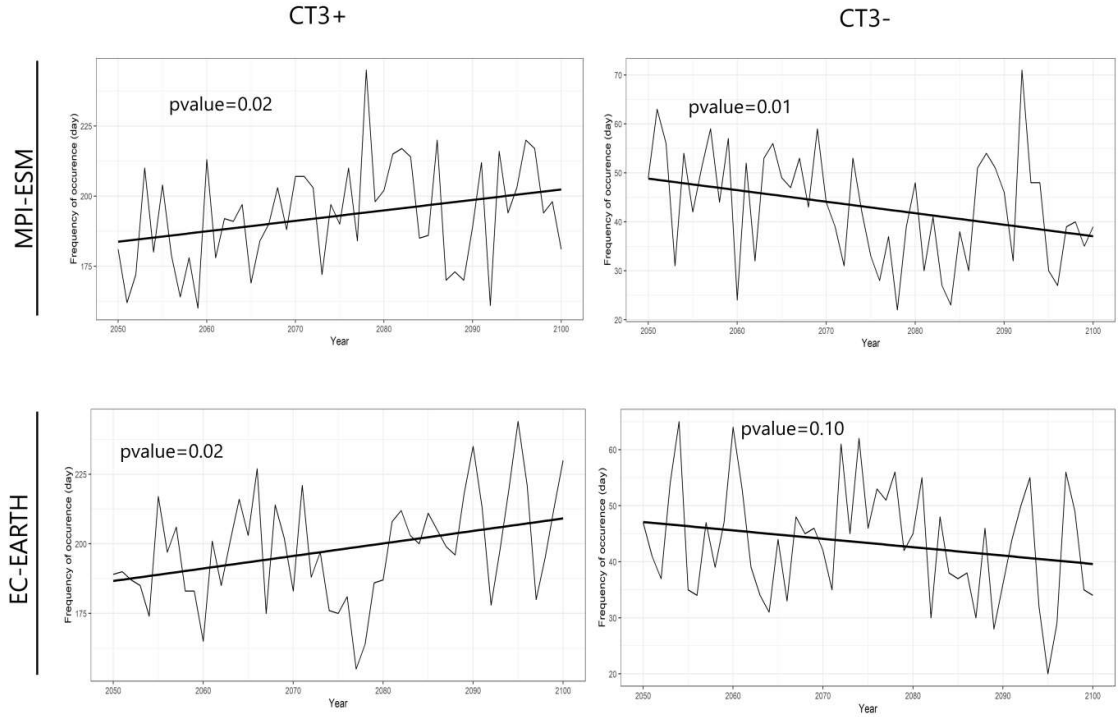

Fig. 12: Simulated trends in CT3+ and CT3- from the GCMs, under the ssp585 scenario for the 2050-2100 analysis period. The pvalue from the Mann-Kendal test is written in the graph.

Preprints (www.preprints.org) | NOT PEER-REVIEWED | Posted: 26 May 2021 doi:10.20944/preprints202105.0631.v1

4 Discussions

This study used circulation typing to examine physically interpretable CTs in Africa south of the equator that can be associated with wet and dry conditions in Western Cape, the relationship between the CTs and the SAM, and changes in the annual frequency of occurrence of the CTs related to the SAM under the ssp585 scenario. Generally, the CTs found to be associated with wet (dry) conditions in Western Cape features (i) low-level cyclonic (anti-cyclonic) relative vorticity and, (ii) the northward (southward) track of westerlies and mid-latitude cyclones. These results are in agreement with the dry and wet patterns of atmospheric circulation over western South Africa reported by Reason and Rouault (2005). Similar results were reported by Gillett and Jones (2006) for landmasses in the southern hemisphere. Also, as found by Mahlalela et al. (2019), subsidence (stable atmosphere) was found to be associated with winter dryness in the (western) parts of Western Cape

Engelbrecht and Landman (2016) found that some synoptic types associated with wet and dry conditions over Western Cape can be linked to the SAM and ENSO. Two of the selected synoptic states in this paper that control rainfall variability of Western Cape, were found to be significantly related to the SAM and ENSO. Among the CTs, the CT dominant during austral summer was found to be related to El Niño. It brings significantly below-average rainfall in some eastern parts of Western Cape. It features a weaker state of the western branch of the Mascarene high, and anticyclonic circulation south of South Africa, suggesting that through this synoptic state, El Niño might cause below-average austral summer rainfall at some eastern parts of Western Cape, especially through the weakening of southeasterly moisture fluxes advected by the western branch of the Mascarene high. The wet CT linked to the SAM is dominant during austral winter and early austral spring; it features the equatorward track of mid-latitude cyclones and brings above-average rainfall in the western regions of Western Cape. Years with below-average SAM index correlate with the above-average frequency of occurrence of the CT.

Studies have indicated that under global warming, the SAM is projected to undergo a trend towards positive polarity during austral summer, due to an increase in greenhouse gas concentrations and stratospheric ozone depletion (Gillett and Thompson 2003). This finding is in agreement with the positive trend found under the ssp585 scenario, in the frequency of occurrence of an austral summer dominant CT (related to the SAM), associated with enhanced SLP at the mid-latitudes, that its occurrence is also enhanced by the positive SAM phase. It was equally found that the frequency of occurrence of the wet austral winter CT related to the SAM significantly decreases under the ssp585 Scenario. Mahlalela et al. (2019) reported a projected decrease in early winter rainfall (which correlates with the SAM) in Western Cape under greenhouse gas warming. The decrease in the frequency of occurrence of the CT might be related to the shift towards positive polarity of the SAM, since on average, the above-average SAM index correlates with the below-average frequency of occurrence of the CT. Thus during austral winter, the southwestern parts of Western Cape might be drier under global warming. This is also in agreement with the study of Burls et al. (2019), that the decrease in the duration of rainfall events associated with cold fronts can be associated with Hadley expansion across the southern hemisphere and post-frontal high-pressure conditions that suppress orographically enhanced rainfall.

Finally, similar results were derived by analyzing the trend in the CTs related to SAM using the CMIP5 GCMs under the RCP.85 scenario. While the year-to-year variations in the annual occurrence of the CTs are subjected to inter-model uncertainties, they agree towards a

 doi:10.20944/preprints202105.0631.v1

tendency of decrease/increase in the annual occurrence of CTs associated with northward/southward track of the mid-latitude cyclones (see Appendix 1).

5 Conclusions

Using obliquely rotated PCA CTs were classified in Africa south of the equator. Four CTs were found to be associated with dry events in Western Cape and three CTs were found to be associated with wet events in Western Cape. The synoptic features of two of the dry CTs reveal that during austral winter, large-scale subsidence and atmospheric blocking of the mid-latitude cyclone, adjacent to South Africa, can be associated with negative rainfall anomaly at western regions of Western Cape. During austral summer, the positioning of the semi-permanent high, south of South Africa, and to some extent, a weaker state of the western branch of the Mascarene high can be associated with austral summer dryness in some eastern parts of Western Cape. Generally, anti-cyclonic circulation south of South Africa brings about dry conditions in Western Cape. Wet days in Western Cape can be associated with reverse synoptic situations, which include: cyclonic circulation south of South Africa, northward track of the mid-latitude cyclones, and the associating band of westerlies. These synoptic situations favor cold fronts to sweep across Western Cape.

One of the selected wet CTs was found to be correlated with the SAM, suggesting that the negative/positive phases of the SAM can be related to atmospheric circulations that favor positive/negative rainfall anomaly in the western parts of Western Cape. Under global warming, a statistically significant negative trend was found in the frequency of occurrence of the (austral winter) wet CT related to the SAM.

Declaration

Conflict of interest: There are no conflicts of interest in this paper

Funding statement: This research received no specific grant from any funding agency in the public, commercial, or not-for-profit sectors.

Preprints (www.preprints.org) | NOT PEER-REVIEWED | Posted: 26 May 2021 doi:10.20944/preprints202105.0631.v1

Appendix

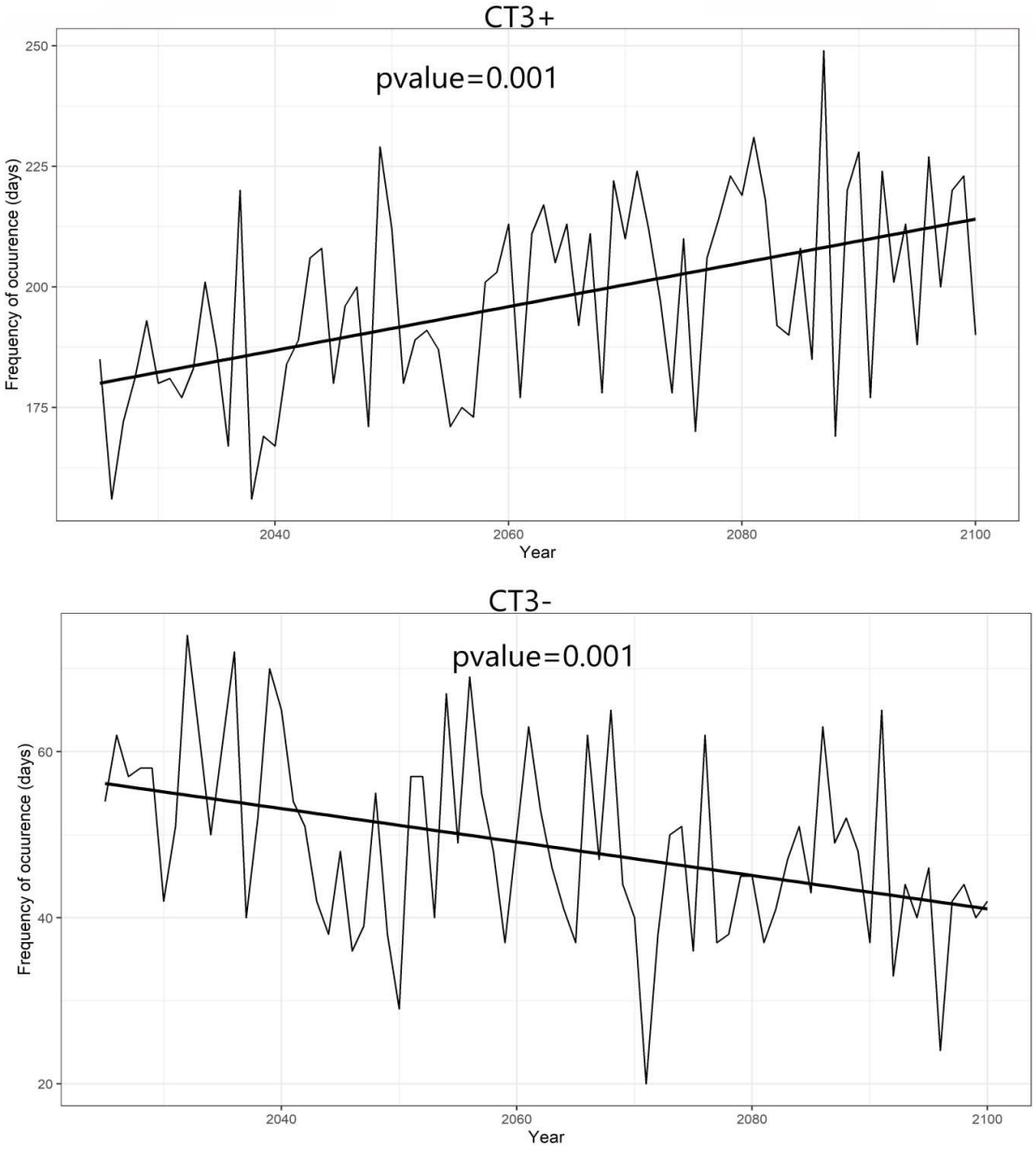

Appendix 1: Trend in the annual frequency of occurrence of CT3+ and CT3- exemplified from the high-resolution CMCC-CMS CMIP5 GCM, for the 2030-2100 period under the RCP8.5 scenario.

References

1. Abram N J, Mulvaney R, Vimeux F, Phipps SJ, Turner J, England MH (2014) Evolution of the Southern Annular Mode during the past millennium. Nat Clim Change 4:564–569. doi: 0.1038/nclimate2235.
2. Barreira S, Compagnucci RH (2011) Spatial fields of Antarctic sea-ice concentration anomalies for summer–autumn and their relationship to Southern Hemisphere atmospheric circulation during the period 1979–2009. Ann Glaciol. 52:140-150.
3. Burls N J, Blamey RC, Cash B A et al (2019) The Cape Town "Day Zero" drought and Hadley cell expansion. Clim Atmos Sci 2, 27 (2019)
4. Cai W, Van Rensch P, Borlace S, Cowan T (2011) Does the Southern Annular Mode contribute to the persistence of the multidecade-long drought over southwest Western Australia? Geophys Res Lett 38 14.
5. Codron F (2005) Relation between annular modes and the mean state: Southern Hemisphere summer. J Clim 18: 320–330.
6. Compagnucci RH, Araneo D, Canziani PO (2001) Principal sequence pattern analysis: a new approach to classifying the evolution of atmospheric systems. Int J Climatol 21: 197–217
7. Compagnucci RH, Richman MB (2008) Can principal component analysis provide atmospheric circulation or teleconnection patterns? Int J Climatol, 28 703–726.
8. Cook KH (2000) The South Indian Convergence Zone and Interannual Rainfall Variability over Southern Africa. J Climate 13:3789–3804.
9. Ding Q, Steig EJ, Battisti DS, Wallace JM (2012) Influence of the Tropics on the Southern Annular Mode. J Clim 25:6330–6348.
10. Gillett NP, Kell TD, Jones PD (2006) Regional climate impacts of the Southern Annular Mode. Geo phys Res Lett 33 23
11. Grassi B, Redaelli G, Visconti G (2005) Simulation of Polar Antarctic trends: Influence of tropical SST. Geophys Res Lett 32 L23806.
12. Hersbach H et al (2020) The ERA5 global reanalysis. Q J R Meteorol Soc 146:1999-204
13. Hendon HH, Thompson DWJ, Wheeler MC (2007) Australian rainfall and surface temperature variations associated with the Southern Hemisphere annular mode. J Clim 20:2452–2467.
14. Hewitson BC, Crane RG (2002) Self organizing maps: applications to synoptic climatology. Clim Res 22:13–26.
15. Huth R (1996) An intercomparison of computer-assisted circulation classification methods. Int J Climatol 16:893-922.
16. Ibebuchi CC (2021a) Can synoptic patterns influence the track and formation of tropical cyclones in the Mozambique Channel? Preprint, available at Research Square. Viewed 19 February 2021, DOI: 10.21203/rs.3.rs-200536/v1
17. Ibebuchi CC (2021b) On the fuzziness of circulation types derived from the application of obliquely rotated principal component analysis to a T-mode climatic

field. Preprint, available at Research Square. Viewed 24 May 2021, DOI:10.21203/rs.3.rs-530514/v1

18. Kalnay E et al (1996) The NCEP/NCAR 40-year reanalysis project. Bull Amer Meteor Soc 77:437-472.
19. Kendall MG (1975) Rank Correlation Methods. Griffin, London, UK
20. Kidson JW (1997) The utility of surface and upper air data in synoptic climatological specification of surface climatic variables. Int J Climatol 17 4:399–414.
21. L'Heureux ML, Thompson DWJ (2006) Observed relationships between the El Niño–Southern Oscillation and the extratropical zonal-mean circulation. J Climate 19: 276–287.
22. Mann HB (1945) Non-parametric tests against trend. Econometrica 13 3:245-259
23. Muller M (2018) Cape Town's drought: don't blame climate change. Nature 559, 174–176.
24. North GR, Bell TL, Cahalan RF, Moeng FJ (1982) Sampling errors in the estimation of empirical orthogonal functions. Mon Wea Rev 110:699–706.
25. Otto F E L et al (2018) Anthropogenic influence on the drivers of the Western Cape drought 2015–2017. Environ Res Lett 13, 124010
26. Philippopoulos K, Deligiorgi D, Kouroupetroglou G (2014) Performance Comparison of Self-Organizing Maps and k-means Clustering Techniques for Atmospheric Circulation Classification. Int J Energy Environ, 8, 171-180.
27. Reason CJC, Rouault M (2005) Links between the Antarctic Oscillation and winter rainfall over western South Africa. Geo phys Res Lett 32 7.
28. Reason CJC, Smart S (2015) Tropical Southeast Atlantic warm events and associated rainfall anomalies over Southern Africa. Front Environ Sci. 3:24.
29. Richman MB (1981) Obliquely rotated Principal Components: an improved meteorological map typing technique? J Appl Meteorol 20:1145–1159.
30. Richman MB, Lamb PJ (1985) Climatic pattern analysis of three and seven-day summer rainfall in the Central United States: some methodological considerations and regionalization. J Climate Appl Meteor. 24:1325–1343.
31. Richman MB (1986) Rotation of principal components. J Climatol 6:293-335.
32. Richman M. B., and X. Gong, 1999: Relationships between the definition of the hyperplane width to the fidelity of principal component loadings patterns. J. Climate. 12:1557–1576.
33. Seager R, Harnik N, Kushnir Y, Robinson W, Miller J (2003) Mechanisms of hemispherically symmetric climate variability. J Clim 16:2960–2978.
34. Screen J, Gillett N, Stevens D, Marshall G, Roscoe H (2009) The role of eddies in the Southern Ocean temperature response to the southern annular mode. J Clim 22:806–818.
35. Thompson DWJ, Wallace JM (2000) Annular modes in the extratropical circulation. Part I: Month-to-month variability. J Clim 13:1000–1016.
36. Wang G, W Cai (2013) Climate-change impact on the 20th-century relationship between the Southern Annular Mode and global mean temperature. Sci Rep 3, 2039.

 doi:10.20944/preprints202105.0631.v1

37. Watterson IG (2001) Zonal wind vacillation and its interaction with the ocean: Implication for interannual variability and predictability. J Geophys Res, 106 (D20) 965–975.

38. Wolski, P (2018) How severe is Cape Town's "Day Zero" drought? Significance 15, 24–27

39. Xie P, Chen M, Yang S, Yatagai A, Hayasaka T, Fukushima Y, Liu C (2007) A gauge-based analysis of daily precipitation over East Asia. J Hydrometeor 8 607:626.